

# INTERNATIONAL SOCIETY FOR SOIL MECHANICS AND GEOTECHNICAL ENGINEERING



*This paper was downloaded from the Online Library of the International Society for Soil Mechanics and Geotechnical Engineering (ISSMGE). The library is available here:*

<https://www.issmge.org/publications/online-library>

*This is an open-access database that archives thousands of papers published under the Auspices of the ISSMGE and maintained by the Innovation and Development Committee of ISSMGE.*



# INTERACTION BETWEEN STRIP FOOTING AND SOFT GROUND TUNNEL

## L'INTERACTION ENTRE LES SUPPORTS ET PASSAGE SOUTERRAIN QUI EST VASCUX

A. Badie<sup>1</sup> M.C. Wang<sup>2</sup>

<sup>1</sup>Vice President, LRA Engineering, Rancho Cordova, California, U.S.A.

<sup>2</sup>Professor of Civil Engineering, Pennsylvania State University, University Park, Pennsylvania, U.S.A.

**SYNOPSIS:** Interactions between strip footings and circular shallow soft ground tunnels were investigated. The analysis was made on an IBM-PC computer using a program named FLAC. The soil was characterized as a non-linear elastic perfectly plastic material. Within the elastic range, the hyperbolic stress-strain law was used, whereas the Drucker-Prager yield criterion was adopted to model the plastic behavior. Variables analyzed included footing displacement, tunnel deformation, stress distribution, displacement field, and ultimate bearing capacity of the footing. These variables were used to evaluate the degree of footing/tunnel interaction.

### 1 INTRODUCTION

Transportation, water, and sewer tunnels as well as utility conduits quite often are constructed in soft ground. Soft ground tunnels may be located near the ground surface. When shallow soft ground tunnels are overlay by buildings, they interact with the building foundations. Interaction between tunnels and foundations affects the stability of both the tunnels and foundations. Thus, to design a safe, economic, and structurally sound soft ground tunnel beneath and the overlying foundation, a proper consideration of the interaction between them is required.

Very few studies on foundation/tunnel interaction are available. There are some studies, however, on the effect of underground cavity (or void) on the performance of overlying footings. Wang and his co-workers (Badie & Wang, 1984; Baus & Wang, 1983; Wang & Baus, 1980; Wang & Badie, 1985; and Wang et al. 1989) reported, based on their finite element analyses, various important factors influencing footing stability. The factors investigated were footing size and configuration; loading condition; cavity condition including cavity size, location, and orientation with respect to the footing; and soil conditions which involves soil property and layer composition. They considered the conditions of a single footing above a single cavity, a single footing above double cavities and double footings above a single cavity (Badie & Wang, 1990, a&b). Other studies such as Wood and Larnach (1985) and Drumm, et al. (1987) reported findings similar to those of Wang and his coworkers. Meanwhile, Abdollah, et al. (1987 a&b) utilized the theory of elasticity to analyze cavity deformation as well as stress distribution around the cavity.

This paper addresses the interaction between strip footings and circular unlined soft ground tunnels for a single footing above a single tunnel, and a single footing above two parallel tunnels. Particular emphases are placed on the analysis of footing and tunnel collapse, displacement velocity-vectors, stress distribution, and the extent of the influence zone.

### 2 INTERACTION ANALYSIS

The interaction between footings and tunnels was analyzed using a two-dimensional finite difference program named FLAC (Itasca, 1987). The foundation soil was a compacted clay having a dry density of 1378 kg/m<sup>3</sup> with a water content of 23%. The soil properties included an internal friction angle of 8 degrees, a unit cohesion of 158.7 KPa, an initial modulus in compression of 19.87 KPa and a Poisson's ratio of 0.39.

The footing/tunnel conditions analyzed are a single footing above a single tunnel for different footing and tunnel sizes with varying tunnel locations, and a single footing above double tunnels with different tunnel spacings, depths to tunnels, and tunnel sizes. The results of computer analysis provide footing settlement, tunnel deformation, stress, strain, and soil yielding. From these data, the footing/tunnel interaction behavior is evaluated for the ultimate loading condition. The ultimate load is determined from the footing pressure versus settlement relationship at the point beyond which the curve reaches a steady minimum slope.

### 3 TUNNEL DEFORMATION/FOOTING SETTLEMENT

According to Badie and Wang (1990a), the vertical displacement of the tunnel crown ( $\delta_c$ ) increases linearly with increasing footing displacement ( $\delta_f$ ). These two displacement values are combined together as a ratio ( $\delta_c/\delta_f$ ), and the entire set of data analyzed are plotted against the ratio of depth to tunnel ( $D$ ) and footing width ( $B$ ), in Figure 1. Note that the data shown in Figure 1 are for a single footing above a single tunnel with the footing width and tunnel diameter each equal to 1 m. The tunnel is either centered with the footing or off-centered having an eccentricity denoted by  $E$  as shown in the inset. The figure illustrates, as would be expected, that the ratio  $\delta_c/\delta_f$  is greatest when the tunnel is centered with the footing. For the  $E/B = 0$  curve, the value of  $\delta_c/\delta_f$  approaches a maximum of 1.0 at the ground surface i.e. at  $D/B = 0$ , and decreases gradually with increasing  $D/B$ . For a constant  $D/B$ , the ratio  $\delta_c/\delta_f$  decreases with increasing  $E/B$ . The figure reveals that the maximum  $\delta_c/\delta_f$  on each curve takes place at a greater depth when  $E/B$  is higher. In other words, for near surface shallow tunnels, the farther away from the footing the smaller the footing/tunnel interaction.

For the condition of a single footing above two parallel tunnels, with  $D/B = 2$  and  $S/B = 4$ , where  $S$  = center-to-center tunnel spacing, the effect of relative position between the footing and the tunnels on footing displacement and tunnel deformation is illustrated in Figure 2. Note that the relative position between footing and tunnel is indicated by  $\alpha$  which is the horizontal distance between footing center and center of double tunnels as illustrated in the inset of Figure 2. It is seen that as the footing moves away from the far tunnel, the tunnel crown displacement decreases, and the crown displacement near the tunnel increases as the footing moves closer to the near tunnel. The footing displacement appears to decrease slightly with increasing  $\alpha$ .

The crown displacement of the near tunnel to the footing displacement ratio is plotted against  $D/B$  for different values of  $\alpha$  in Figure 3. The

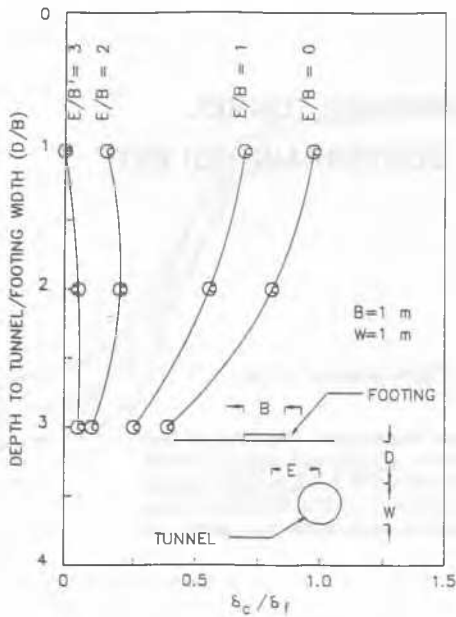


Figure 1: Vertical displacement ( $S/S_i$ ) vs. depth ( $D/B$ ).

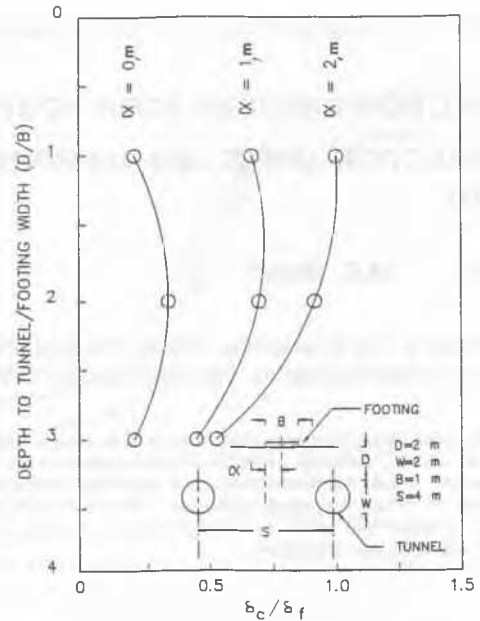


Figure 3:  $S_i/S_i$  vs  $D/B$  for the near tunnel.

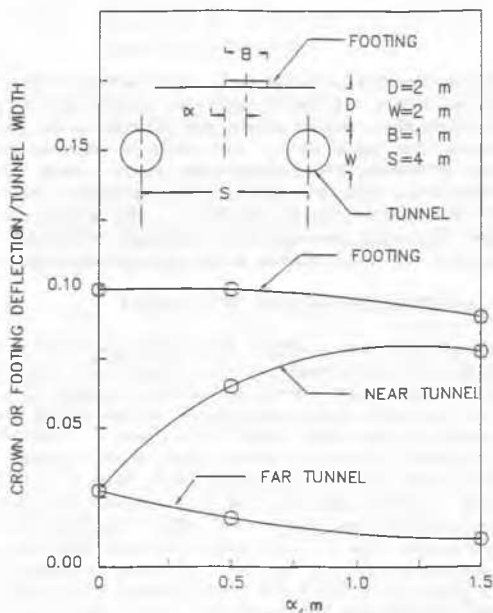


Figure 2: Displacements vs. distance.

shape of the curves resembles that of Figure 1. The difference is entirely caused by the presence of the adjacent tunnel. As expected the presence of the adjacent tunnel results in a greater ratio of  $\delta_c/\delta_f$  when compared with the condition of a single footing over a single tunnel.

#### 4 STRESS DISTRIBUTION

The vertical stress distribution caused by soil weight and footing load for a single footing centered above double tunnels is shown in Figure 4 along four vertical planes. The four planes are at footing center, at the center of a tunnel, and at each edge of the tunnel. The inset of the figure shows the locations of the four vertical planes and the dimensions and configurations of the footing and tunnels. The distribution curve for the footing center shows an abrupt increase in stress immediately above the crown level of the tunnels, followed by a sharp decrease. Such a variation in stress distribution can be attributed to soil arching effects.

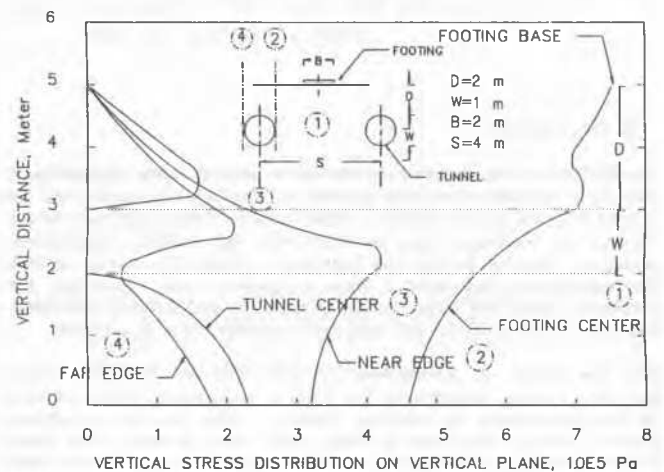


Figure 4: Vertical stress distributions on vertical planes.

Without the tunnels, the shape of the curve is expected to follow that of Boussinesq distribution. Among the other three curves, all starting from zero at the ground surface, the vertical stress along the tunnel center line increases with depth faster than the other two lines, then drops abruptly to zero at the tunnel crown. Below the tunnel bottom, the vertical stress increases with depth at a decreasing rate. At both tunnel edges, the vertical stress undergoes a sharp increase, followed by an abrupt decrease across the height of the tunnel. The stress at the tunnel edge near the footing (near edge) is greater than that of the far edge primarily because the near edge is under a greater influence of the footing load.

The vertical stress distributions along the horizontal planes, one each at top, mid-height, and bottom of the tunnels are illustrated in Figure 5. Note that because of symmetry, only one-half of the distribution curves is presented. Between the right edge of the tunnel and the footing center, the vertical stress decreases with increasing horizontal distance from a maximum at footing center, resembling the typical distribution curve for no-tunnel condition. As expected, at the footing center, the vertical stress is greatest at the top and smallest at the bottom level of the tunnel. Near the tunnel edge, however, the stress at the top becomes much smaller than that at the bottom, and the stress at mid-height is essentially equal to that at the bottom. Far away from the

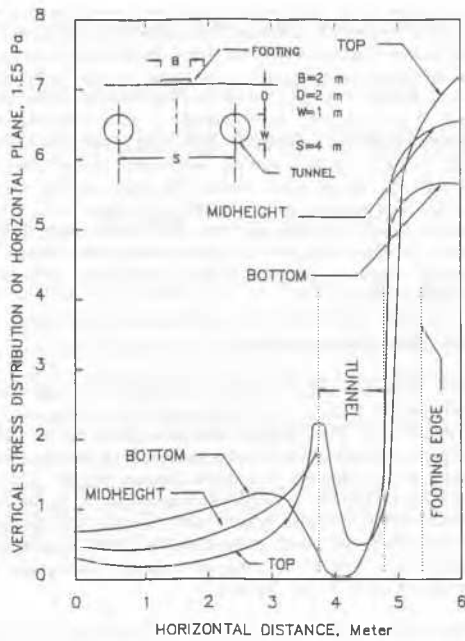


Figure 5: Vertical stress distribution on horizontal planes.

other edge of the tunnel, the vertical stress decreases with increasing horizontal distance, and the magnitude is greatest at the bottom and smallest at the top. This is as would be expected because far from the footing load, the vertical stress is predominantly caused by the soil weight which increases with increasing depth. Within the diameter of tunnel, the vertical stress both at the top and the bottom levels undergoes abrupt changes. At top level, the vertical stress decreases and increases abruptly at the tunnel indicating a high degree of interaction between the footing and the tunnel.

The major principal stress contours for a single footing centered above double tunnel is presented in Figure 6. It is seen that the greatest major principal stress develops at footing edges, and that the stress decreases gradually with increasing depth. As would be expected, the major principal stress at the tunnel is much smaller than that at the footing. The figure also demonstrates stress concentrations at footing edges and also at the top of the tunnel. It is expected that soil yielding will initiate from the high stress concentration area then gradually propagate downward toward the tunnel area.

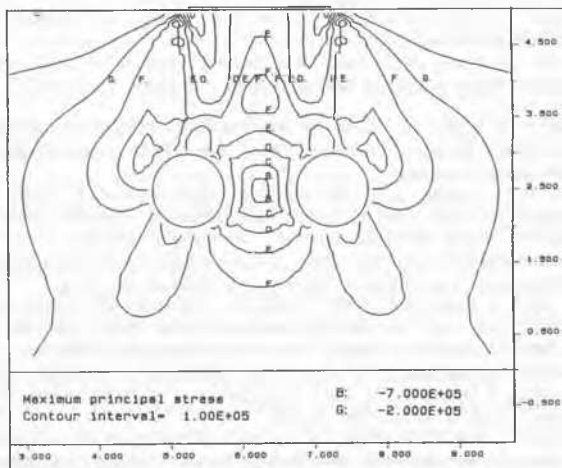


Figure 6: Major principal stress contours.

## 5 DISPLACEMENT FIELD

As the footing load increases, soil yielding which initiates from the footing edges will propagate downward and laterally. Depending on the size and location of the tunnel, the soil yielding may or may not reach the tunnel before the footing collapses. The displacement field at footing collapse differs for different footing and tunnel conditions as illustrated in Figures 7 and 8. Figure 7 demonstrates the variation of displacement velocity vectors with footing size for a constant tunnel size and depth to tunnel, each equal to 2 m. The four footing sizes shown are 0.16, 0.54, 1.0 and 1.92 m. According to the figure, when the footing size is very small compared to the tunnel size, the velocity field is dominated by lateral and upward vectors signifying a general shear failure in the foundation soil when the footing collapses. As the footing size increases, the velocity vector orients toward the tunnel suggesting a punching shear failure in which the soil underneath the footing is pushed by the footing into the tunnel. When the footing size is larger than the tunnel size, the yielding soil mass is wider than the tunnel, thus involving some radial shear failure at the tunnel shoulder. For the condition of footing size equal to the tunnel size, such as that shown in Figure 8, the mode of failure changes from punching shear at shallow depths to general shear at greater depths. The transition of soil failure mode with increasing depth to tunnel is clearly depicted in Figure 8.

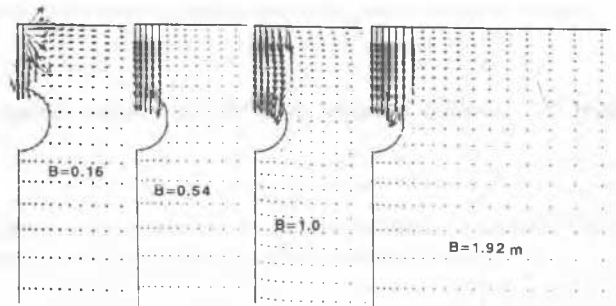


Figure 7: Displacement velocity vectors for four footing sizes.

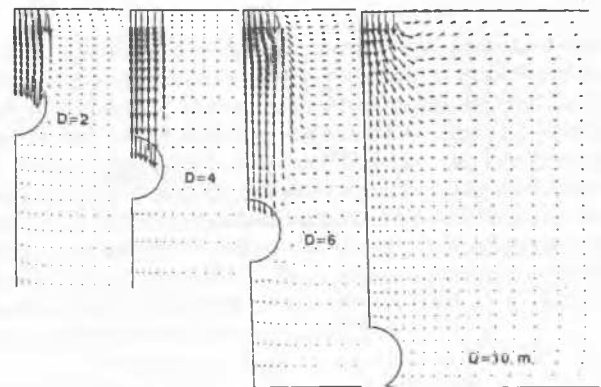


Figure 8: Displacement velocity vectors for four depths to tunnel.

## 6 BEARING CAPACITY

For a single footing centered above a single tunnel of a constant size and a constant depth to tunnel, the ultimate bearing capacity of the footing varies with footing width. Figure 9 presents such a variation for two levels of depth to tunnel. The conditions analyzed involve a varying footing width (B) with  $W = 1$  m and  $D = 1$  and 2 m. The ultimate bearing capacity for each condition analyzed is expressed as a percentage of the ultimate bearing capacity for a no-tunnel condition. The figure demonstrates that as the B/D ratio increases within the range of conditions analyzed, the bearing capacity decreases from a maximum of 100% at a very small B/D to a minimum at B/D of about 1.0, then increases gradually. The drop in ultimate bearing capacity is much greater for  $D = 1$  m than  $D = 2$  m; the minimum value of bearing capacity at  $B/D = 1.0$  equals 42% for  $D = 1$  m and 62% for  $D = 2$  m.

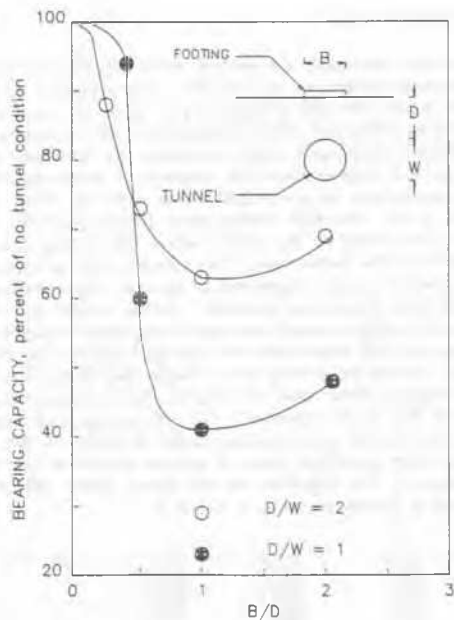


Figure 9: Bearing capacity vs. (D/B) for circular tunnel.

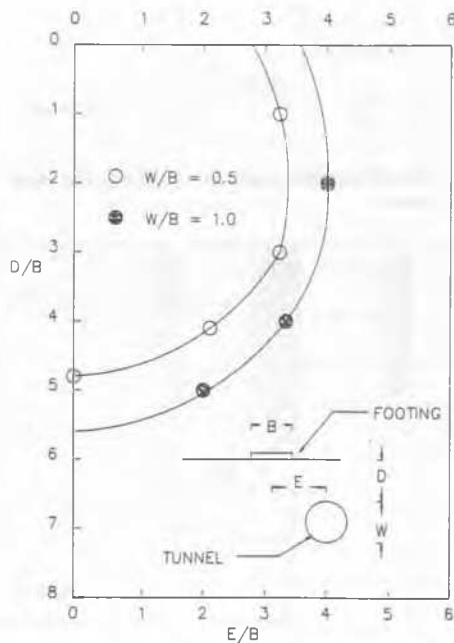


Figure 10: Critical zone for single footing above single tunnel.

The high value of bearing capacity with smaller footings can be attributed to the result of general shear failure, while the lower bearing capacity with larger footings may be a result of punching and/or local shear failure. The general shear failure involves displacement of the yielded soil mass to the ground surface, whereas, in the punching shear failure, the soil mass underneath the footing displaces vertically into the cavity. At  $B/D=2$ , because the footing size is much greater than the tunnel, a punching shear failure is unlikely to occur. Instead, a local shear failure involving a tunnel size collapse may take place. As a result, the bearing capacity becomes greater than that of  $B/D=1$ . When the two minimum bearing capacity values at  $B/D=1$  are compared, the greater value of 62% for  $D=2$  m can be attributed to the fact that at  $B/D=1$  the footing size,  $B=1$  m, is twice the tunnel size, which reduces the effect of punching shear.

For the same tunnel size and depth to tunnel, footing/tunnel interaction decreases as the eccentricity between footing and tunnel increases. The degree of interaction may be evaluated from the ultimate bearing capacity value, since interaction results in a decrease in the ultimate bearing capacity of the footing. Thus, based on the analyzed ultimate bearing capacity data, it is possible to establish a zone beyond which the presence of the tunnel has negligible interaction with the footing. The extent of such a zone under a footing, hereinafter termed as the critical zone, varies with the tunnel size. Figure 10 presents the extent of the critical zone for two tunnel sizes of  $W/B=0.5$  and  $1.0$ . The figure demonstrates, as would be expected, that the critical zone is greater for a larger tunnel. When the tunnel is located within the critical zone, the ultimate bearing capacity of the footing decreases with decreasing distance from the tunnel.

## 7 SUMMARY AND CONCLUSIONS

The interaction between strip footings and shallow circular soft ground tunnels was investigated using a two dimensional finite difference computer program named FLAC. The analysis was performed on an IBM-PC. In the analysis, the soil was idealized as a nonlinear elastic perfectly plastic material which obeys Hooke's law and Drucker Prager yield criterion. Conditions analyzed included a single footing above a single tunnel and a single footing above double tunnels with varying footing and tunnel sizes, tunnel locations, and depth to tunnels. Variables investigated were footing displacement, tunnel deformation, stress distribution, and the ultimate bearing capacity of the footing.

Based on the results of the study, it is concluded that significant footing/tunnel interaction will take place only when the footing and tunnel are located within the critical zone. The extent of the critical zone varies with the tunnel size. The closer the tunnel is to the footing, the greater the interaction will be. The interaction will result in greater footing displacements and tunnel deformations, and will decrease the ultimate bearing capacity of the footing. Thus, to design a safe and structurally sound soft ground tunnel and the overlying footing, the interaction between the two must be properly taken into consideration.

## REFERENCES

- Abdellah, G.A.H. & Abdalla, M.H., 1987/a. The Interaction Between a Tunnel/Cavity and Nearby Structures. Proc. VI Aust. Tunnelling Conf. (1): 183-189.
- Abdellah, G.A.H., Abdalla, M.H., & A.E.N. Dil, 1987/b. Study of Soil Media with Multiple Tunnels or Cavities Using the Boundary Element Techniques. Proc. VI Aust. Tunnelling Conf. (1): 193-200.
- Badie, A. & Wang, M.C., 1984. Stability of Spread Footing Above Void in Clay. J. Geol. Eng. (ASCE) 110 (11): 1591-1605.
- Badie, A. & Wang, M.C., 1990a. Response of Underground Cavity to Surface Loading. Proc. Int. Cong. on Tunnel & Underground Works.
- Badie, A. & Wang, M.C., 1990b. Stability of Underground Cavity Subjected to Surface Loads. Proc. Int. Symp. on Unique Underground Structures.
- Baus, R.L. & Wang, M.C. 1983. The Bearing Capacity of Strip Footing Located Above a Void in Cohesive Soils. J. Geol. Eng. (ASCE) 109 (11): 1-14.
- Cundall, P. & Board, M., 1988. A Microcomputer Program for Modeling Large-Strain Plasticity Problems. Proc. 6th Intl. Conf. on Numerical Methods in Geomech.
- Drumm, E.C., Ketelle, R.H., Manrod, W.E., Ben-Hassine, J., 1987. Analysis of Plastic Soil in Contact with Cavitose Bedrock. Geot. Prac. for Waste Disposal, Sp. Pub. 13, ASCE: 418-431.
- Itasca Consulting Group, Inc. 1987. FLAC: Fast Lagrangian Analysis of Continua. User Manual, Version 2.0, Minneapolis, Minn.
- Wang, M.C. & Baus, R.L., 1980. Settlement Behavior of Footing Above a Void. 2nd Conf. on Ground Movements and Struct: 168-184.
- Wang, M.C. & Badie, A., 1985. Effect of Underground Void on Foundation Stability. J. of Geol. Eng. (ASCE) 111 (8): 1008-1019.
- Wang, M.C. & Hsieh, C.W., 1987. Collapse Load of Strip Footing Above Circular Void. J. Geol. Eng. (ASCE) 113 (5): 511-515.
- Wang, M.C., Yoo, C.S., Hsieh, C.W., 1989. Effect of Void on Footing Behavior Under Eccentric and Inclined Loads. ASCE Foundation Engineering: Current Principles and Practices 2: 1226-1239.
- Wood, L.A. & Larhach, W.J., 1985. The Behavior of Footings Located Above Voids. Pro. 11th Intl. Conf. SMFE (4): 2273-2276.